ARTICLE OPEN

Check for updates

A transcriptional program associated with neurotransmission in the living human brain

Alexander W. Charney[1]✉, Lora E. Liharska[1], Eric Vornholt[1], Alissa Valentine[1], Anina Lund[1], Alice Hashemi[1], Ryan C. Thompson[1], Terry Lohrenz[2], Jessica S. Johnson[1], Nicole Bussola[1], Esther Cheng[1], You Jeong Park[1], Salman Qasim[1], Alisha Aristel[1], Lillian Wilkins[1], Kimia Ziafat[1], Hannah Silk[1], Lisa M. Linares[1], Brendan Sullivan[1], Claudia Feng[1], Seth R. Batten[2], Dan Bang[2,3,4,5], Leonardo S. Barbosa[2], Thomas Twomey[2], Jason P. White[2], Marina Vannucci[6], Beniamino Hadj-Amar[6,7], Emily Moya[1], Martijn Figee[1], Girish N. Nadkarni[1], Michael S. Breen[1], Kenneth T. Kishida[8], Joseph Scarpa[1], Eric E. Schadt[1], Ignacio Saez[1], P. Read Montague[1,4], Noam D. Beckmann[1,9] and Brian H. Kopell[1,9]

At the foundation of neurotransmission, and by extension at the foundation of brain function, are coordinated programs of gene expression involving many thousands of genes. These programs are poorly defined in humans because most modern studies that characterize human brain gene expression use tissue obtained in the postmortem state when neurotransmission and brain function have ceased. Here, to advance knowledge of the gene expression programs at the foundation of neurotransmission in the human brain, gene expression was characterized in 130 prefrontal cortex (PFC) samples obtained from participants of the Living Brain Project (LBP) during neurosurgical procedures in conjunction with intracranial recordings of neurotransmission traits in deep brain structures. In a group of 15 procedures, participants performed a cognitive task during intracranial recordings of the substantia nigra; in the remaining group of 115 procedures, participants were at rest during intracranial recordings of either the subthalamic nucleus or the globus pallidus. Analyses of the data obtained from the group of 15 procedures, though underpowered to identify individual gene-trait associations, uncovered evidence of transcriptome-wide signatures of PFC gene expression that associated with neurotransmission traits. These signatures were reproduced in analyses of data from the group of 115 procedures and in analyses of data from a third independent human cohort. A set of genes with evidence of association to neurotransmission in multiple cohorts was termed the "transcriptional program associated with neurotransmission" (TPAWN) and analyses of data from studies of model systems and genetic variation in human populations validated the role of TPAWN genes in neurotransmission and brain function. In PFC excitatory neurons of LBP participants, higher expression of TPAWN genes tracked with higher expression of genes that in mouse frontal cortex are markers of excitatory neurons that connect the frontal cortex to deep brain structures. Taken together, the findings of this report help advance knowledge of the transcriptomic foundations of neurotransmission in the living human brain.

Molecular Psychiatry (2026) 31:2727–2738; https://doi.org/10.1038/s41380-025-03420-3

INTRODUCTION

An aim of brain research is to advance knowledge of how human brain functions arise from brain tissue. In this report, the phrase "brain function" is used to refer to capabilities of the brain that emerge from neurotransmission (i.e., the coordinated electrical transfer of information between neurons arranged in neural circuits). Defined this way, brain functions include cognition, perception, emotion, memory, movement, and behavior. Generally speaking, tissue functions originate from genes, which are specialized sequences of deoxyribonucleic acid (DNA) that are transcribed into messenger ribonucleic acid (RNA) transcripts, which are then translated into proteins [1]. Ultimately, at the foundation of tissue functions are an untold number of coordinated processes involving the expression of many thousands of genes that in this report are referred to as the "transcriptomic foundations" of tissue function [2]. In human brain tissue, transcriptomic foundations set the stage for neurotransmission, and from complex patterns of neurotransmission involving the prefrontal cortex (PFC) and other brain areas emerge brain functions [3]. These functions go awry in brain illnesses.

Historically, studies of living humans during neurosurgical procedures have played a key role in establishing what is currently known about how brain functions emerge from brain tissue. For example, studies during neurosurgical procedures performed by Wilder Penfield resulted in the development of the cerebral homunculus that is used in neuroscience education to teach the anatomical basis of brain functions [4, 5]. Modern technologies such bulk RNA sequencing (bulk RNA-seq; i.e., the capture and

[1]Icahn School of Medicine at Mount Sinai, New York, NY, USA. [2]Virginia Tech, Roanoke, VA, USA. [3]Aarhus University, Aarhus, Denmark. [4]University College London, London, UK. [5]University of Oxford, Oxford, UK. [6]Rice University, Houston, TX, USA. [7]University of South Carolina, Columbia, SC, USA. [8]Wake Forest School of Medicine, Winston-Salem, NC, USA. [9]These authors contributed equally: Noam D. Beckmann, Brian H. Kopell. ✉email: alexander.charney@mssm.edu

Received: 7 March 2025 Revised: 6 November 2025 Accepted: 2 December 2025
Published online: 19 February 2026

A) Data collection procedures

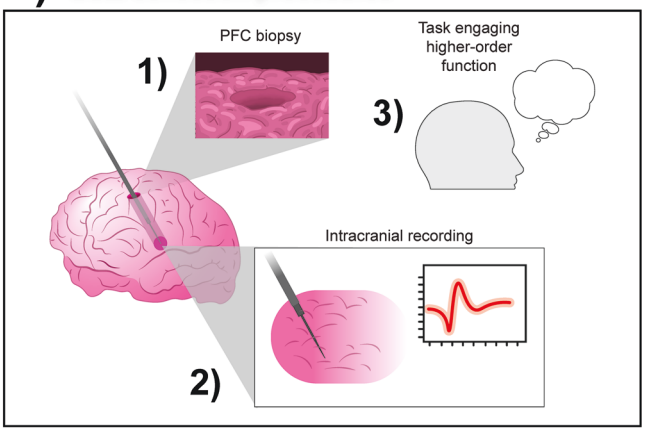

B) Study cohort

	LIV	PM
Individuals	**104**	**20**
Mean age in years	61.65 (24-84)	67.65 (33-84)
Male:female	64:40	12:8
Affected:unaffected (PD)	91:13	9:11
PFC samples analyzed		
Single-nucleus RNA-seq	*31*	*20*
FCSV differential expression	15	0
LIV-PM differential expression	13	20
TPAWN Npr3 annotation	31	0
Bulk RNA-seq	*115*	*0*
MER differential expression	115	0

Fig. 1 Overview of Study. (**A**) Data collection procedures. Schematic illustrating how prefrontal cortex (PFC) biopsies are obtained in conjunction with intracranial electrical recordings. In 1) the state of the PFC after the biopsy is obtained is depicted. In 2) a probe obtaining electrical recordings from deep brain structures is depicted. In 3) a cartoon of a person is shown to illustrate that in some cases while electrical recordings are obtained the study participant is engaged in a cognitive task. (**B**) Study cohort. Numbers refer to sample size (i.e., individuals or samples) except for age. Sample sizes are shown for most of the analyses of LBP data presented in the report. Affected/unaffected refers to whether the individual is affected with Parkinson's disease (PD) or not (e.g., unaffected individuals underwent DBS for other indications).

quantification of pooled RNA from the cells of a sample) and single-nucleus RNA sequencing (snRNA-seq; i.e., the capture and quantification of RNA from many individual nuclei in a tissue sample) allow researchers to characterize the transcriptome of human brain tissue. Despite the widespread use of these technologies in human brain research, the transcriptomic foundations of neurotransmission, and by extension the transcriptomic foundations of brain functions, remain poorly characterized in humans. This is, in part, because most of the studies that characterize the transcriptome of human brain tissue use tissue obtained in the postmortem state [6–11], which is defined by the cessation of neurotransmission and function [12].

For the Living Brain Project (LBP), a safe, ethical, and scalable procedure was developed to acquire PFC tissue from living humans for biomedical research purposes (Fig. 1) [13–16]. In previous LBP reports, RNA sequencing of PFC tissues characterized the living human PFC transcriptome [14] and intracranial measurements of neurotransmission performed while study participants played a computer game revealed patterns of dopamine and serotonin neurotransmission associated with social cognition [17]. Considered together, these prior LBP reports – along with recent reports from other research groups [18, 19] – highlight the opportunities to advance knowledge of human brain biology that arise when neuroscience research activities are creatively integrated into modern neurosurgical practice. Here, these opportunities are leveraged to address the following question: "Is there a reproducible gene expression signature associated with measures of neurotransmission obtained from the brain of living humans?" To address this question, RNA sequencing data from PFC samples obtained from 130 neurosurgical procedures was combined with measures of neurotransmission obtained intracranially from deep brain structures at the time of PFC sampling, in some cases while participants performed a cognitive task (Fig. 1).

RESULTS

Study cohort

As described previously [13, 14], a procedure was developed for the LBP to obtain PFC samples for research purposes during neurosurgical procedures for deep brain stimulation (DBS), an elective treatment for neurological and mental illnesses [20]. A total of 146 PFC biopsies ("LIV samples") from 104 living participants were studied for the current report, including unilateral biopsies from 62 participants (39 from the left hemisphere and 23 from the right hemisphere) and bilateral biopsies from 42 participants. The majority of samples were obtained from individuals with Parkinson's disease (PD), the most common indication for DBS (Fig. 1).

The analyses presented in the current report center around the following four LBP datasets (Fig. 1B): (1) single-nucleus RNA sequencing (snRNA-seq) data from a total of 31 LIV samples and 20 samples obtained from postmortem donors ("PM samples") introduced in the LBP report by Vornholt et al. [21]; (2) neurotransmission data measured intracranially using fast-scan cyclic voltammetry (FSCV) during 15 DBS surgeries, a subset of which was introduced in the LBP report by Batten et al. [17]; (3) bulk RNA-seq data from 115 LIV samples, which is a subset of the data introduced in the LBP report by Liharska et al. [14]; (4) neurotransmission data measured intracranially using microelectrode recordings (MERs) in these 115 DBS surgeries (this dataset is introduced in the current report). Each of these four LBP datasets is more fully described in the LBP report that first introduced the dataset (when applicable), the respective section of the current report that first describes results of analyses of the dataset, and/or in the methods section of the current report. The details regarding the procedures used for data quality control and statistical modeling of these data are fully described in the methods section of the current report. All of the PFC samples studied in the current report have been studied in at least one previous LBP report.

Analytic approach and key terms

In living individuals, neurotransmission can be measured directly in the brain during neurosurgical procedures using a variety of intracranial electrical recording devices. When such recordings are obtained in conjunction with a brain tissue biopsy, "differential expression" (DE) analysis can be performed to characterize the association between intracranial electrical recording measurements and the expression levels of individual genes. In DE analysis, for a given set of genes (e.g., all genes expressed in a given cell type in snRNA-seq data), the expression level of every gene is tested for association with a trait of interest using a regression model. For a given gene, the regression model beta (by convention, the "logFC" value) for the trait of interest captures both the magnitude and direction of the gene-trait association. In this report, the set of gene-trait logFCs for all genes tested in a DE analysis is referred to as the "DE signature" of the trait, and genes

defined as having statistically meaningful associations with the trait are referred to as "differentially expressed genes" (DEGs). As will be seen below, for the purposes of downstream analyses, when no or few DEGs are identified using adjusted p-values, unadjusted p-values are used to define DEGs in conjunction with orthogonal validation (see discussion section).

The strategy used in this study to investigate whether there is a reproducible gene expression signature associated with measures of neurotransmission obtained from the brain of living humans was to integrate results from "neurotransmission DE analyses" (i.e., DE analyses where the traits of primary interest are intracranial electrical recording measurements). Specifically, neurotransmission DE analyses from three independent cohorts were integrated: (1) a LBP cohort where FSCV was used to measure intracranial neurotransmission; (2) a LBP cohort where MERs were used to measure intracranial neurotransmission; (3) a cohort from a study published by Berto et al. [19] where intracranial electroencephalography (iEEG) was used to measure intracranial neurotransmission. Below, the DE signatures and DEGs resulting from these three types of neurotransmission DE analyses will be referred to by the technique used to measure neurotransmission (e.g., "FSCV DE signature," "FSCV DEGs"). DEGs with positive associations between gene expression and neurotransmission metrics will be referred to below as "Up DEGs" (e.g., "iEEG Up DEGs") and DEGs with negative associations between gene expression and neurotransmission metrics will be referred to below as "Down DEGs" (e.g., "iEEG Down DEGs").

Identification of FSCV DE signatures

FSCV is a method for measuring the fluctuations of dopamine, serotonin, and norepinephrine concentrations in human brain tissue [22–28]. For the current report, FSCV recordings were made during 15 DBS surgeries while study participants (N = 9) played 60 rounds of the ultimatum game [29, 30] approximately 10 min after a PFC biopsy was obtained. The FSCV recordings were made from the substantia nigra pars reticulata (SNr), a deep brain structure with direct white matter connections to the PFC in humans [31, 32]. In the ultimatum game, the participant must decide whether to accept or reject monetary offers from an avatar (the "proposer"). In each round, the proposer offers a split of $20 to the participant that could range from $1 to $9. If the study participant accepts the offer, they get the offered amount and the proposer gets the remaining amount (i.e., the difference between $20 and the offer). If the participant rejects the offer, neither the participant nor the proposer receives any money. The ultimatum game engages brain functions such as social reasoning (e.g., determining what constitutes a fair or unfair offer).

From each of the 15 FSCV recordings, a metric was derived for dopamine, serotonin, and norepinephrine signals by calculating the beta coefficient from a linear model testing the association between fluctuations of the neurotransmitter and the size of the offer made by the proposer to the participant. snRNA-seq was performed on the 15 PFC biopsies obtained in the minutes prior to FSCV recordings, and after the completion of snRNA-seq data quality control procedures 48,735 cells annotated to six brain cell types remained for analysis (19,817 excitatory neurons [Exc]; 4,899 inhibitory neurons [Inh]; 16,062 oligodendrocytes [Oli]; 4,316 astrocytes [Ast]; 2,342 microglia [Micro]; 1,299 oligodendrocyte progenitor cells [OPCs]). For each cell type, DE was performed testing the association between the expression of each RNA transcript detected in that cell type with each of the three neurotransmitters, resulting in a total of 18 FSCV DE signatures. Three FSCV DEGs were identified when using adjusted p-values to define DEGs (the full 18 FSCV DE signatures discovered in this report are provided in Supplementary Table 1). However, using the π_1 statistic [33], which provides a lower bound of the proportion of RNA transcripts tested that truly deviate from the null hypothesis of no association between RNA transcript expression and the DE trait of interest (e.g., the FSCV metric), it was estimated that with larger samples sizes true FSCV DEGs would be identified (i.e., $\pi_1 > 0$) for 13 of the 18 FSCV DE signatures (Fig. 2). The FSCV DE signature with the strongest signal (i.e., the greatest π_1 statistic) was the FSCV DE analysis of dopamine measurements and excitatory neuron RNA transcript expression ("dopamine Exc FSCV DE analysis"; $\pi_1 = 0.41$; Fig. 2). All of the downstream analyses of FSCV DE signatures in this report only utilized "high-confidence" FSCV DE signatures, which were defined as those with a π_1 statistic greater than 0.10 (Fig. 2; Supplementary Figures 1, 2), and a nominally significant p-value (unadjusted p-value < 0.05) was used to define FSCV DEGs in these signatures.

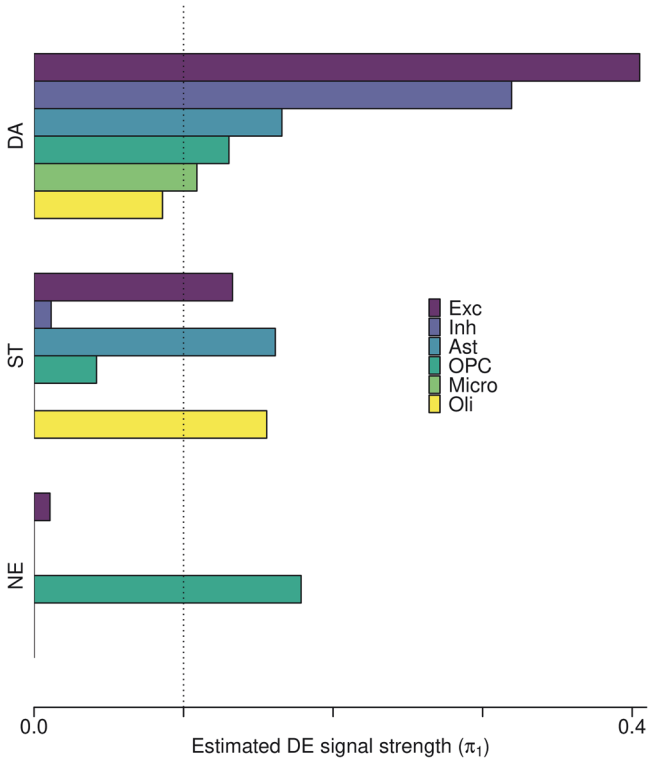

Fig. 2 Bar plot summarizing the results of the 18 FSCV DE analyses. The result of each DE analysis is summarized by the π_1 statistic (x-axis), which provides a lower bound of the proportion of RNA transcripts tested that truly deviate from the null hypothesis of no association between RNA transcript expression and the FSCV metric indicated on the y-axis. For each FSCV metric (i.e., each neurotransmitter) there is a result (a bar) shown for DE of that metric performed in each of 6 cell types (represented by different colors) in the snRNA-seq data.

Validation of FSCV DEG sets defined using unadjusted p-value thresholds

Due to the high rate of false positives introduced when defining DEGs using unadjusted p-value thresholds, any specific gene-trait association defined in this manner may or may not be meaningful. For this reason, the downstream analyses of FSCV DE signatures focused only on establishing that FSCV DEG sets defined in this manner – not specific FSCV DEGs defined in this manner – captured true biological signal.

As a first step towards this end, biological pathways enriched in FSCV DEG sets were identified using the Kyoto Encyclopedia of Genes and Genomes (KEGG) database, which groups genes into sets based on curated annotations from public resources and published literature [34]. KEGG enrichment was performed on the two DEG sets from each of the high-confidence FSCV DE

signatures (i.e., Up DEGs and Down DEGs). After multiple testing correction, a total of 19 associations were found between a KEGG set and a FSCV DEG set (16 unique KEGG sets were found to be enriched in at least one FSCV DEG set [three KEGG sets were enriched in more than one FSCV DEG set]). The 16 KEGG sets in these associations were 'glutamatergic synapse,' 'serotonergic synapse,' 'GABAergic synapse,' 'cholinergic synapse,' 'long-term potentiation,' 'long-term depression,' 'ion channels,' 'neuroactive ligand-receptor interaction,' 'circadian entrainment,' 'retrograde endocannabinoid signaling,' 'oxytocin signaling pathway,' 'GnRH secretion,' 'chromosome and associated proteins,' 'spliceosome,' 'exosome', and 'protein kinases' (full KEGG enrichment statistics for the high-confidence FSCV DE signatures are provided in Supplementary Table 2).

A permutation analysis was performed to confirm that the 19 enrichments observed between a KEGG set and a FSCV DEG set were not spurious associations resulting from the use of unadjusted p-values to define FSCV DEG sets. For each of the 19 enrichments, the following six-step procedure was performed (to help explain certain steps, the enrichment between dopamine Exc FSCV Down DEGs and the KEGG set 'ion channels' [OR = 3.61, p-value = 1.65×10^{-10}] will be referred to as "the illustrative example"):

1. *B* was defined as the set of genes in the FSCV DE analysis. In the illustrative example, *B* was defined as the ~10,000 genes in the dopamine Exc FSCV DE analysis.
2. *N* was defined as the number of FSCV DEGs in *B*. In the illustrative example, *N* was defined as 917 (i.e., the number of genes defined as a Down DEG in the dopamine Exc FSCV DE analysis when using unadjusted p-values to define DEGs).
3. *R* was defined as a set of *N* genes randomly selected from *B*. In the illustrative example, *R* was defined by randomly selecting 917 genes from the ~10,000 genes in *B*.
4. *R* was tested for enrichment of the KEGG gene set using a Fisher's exact test, and the permuted effect size for the enrichment was defined as the resulting OR. In the illustrative example, the 917 genes in *R* were tested for enrichment of the 314 genes in the ion channel KEGG set, and the permuted effect size was 0.89.
5. Steps 2-4 were repeated 10,000 times.
6. An empirical p-value was calculated as the fraction of the 10,000 permuted effect sizes that were more pronounced than the observed effect size (i.e., the effect size reported in column J of Supplementary Table 2).

For all of the 19 observed enrichments, the resulting empirical p-value was less than 2×10^{-4}. Since most of the 16 KEGG sets involved in the 19 observed enrichments were related to neurotransmission (e.g., 'ion channels,' 'long-term potentiation'), this analysis suggests that the FSCV DEG sets defined using unadjusted p-value thresholds were not random noise and captured biological processes involved in neurotransmission.

FSCV DE signatures capture core component of living PFC transcriptome

The KEGG enrichment analysis results presented in the previous section led to the hypothesis that core components of the living human PFC transcriptome may be captured by the high-confidence FSCV DE signatures. To test this hypothesis, the high-confidence FSCV DE signatures were compared to DE signatures differentiating LIV samples from PM samples (Fig. 1B). DE of "LIV-PM status" (i.e., whether a PFC sample is a LIV sample or a PM sample) was performed for each cell type in snRNA-seq data from 13 LIV samples and 20 PM samples and the concordance between the 9 high-confidence FSCV DE signatures and the resulting LIV-PM DE signatures was assessed. The 13 LIV samples

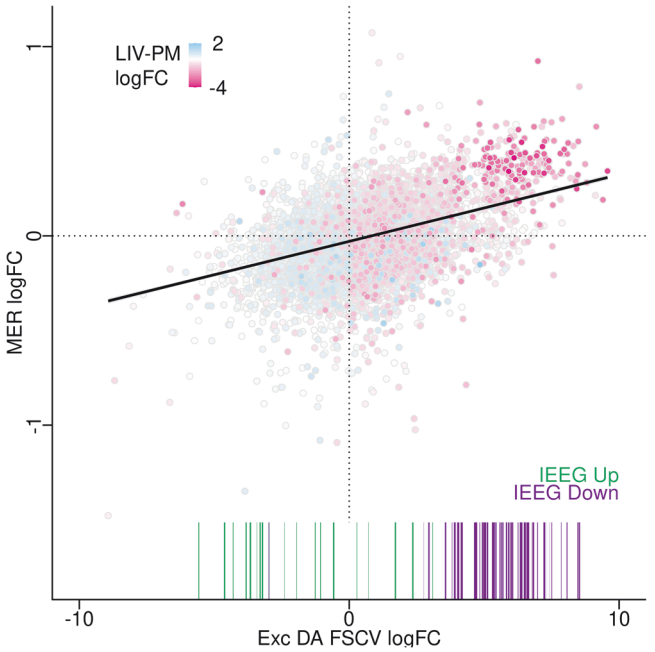

Fig. 3 Scatter plot showing relationship of the logFC values from the FSCV DE signature with the greatest signal strength in panel A (x-axis) to the logFC values from the STN MER DE signature (y-axis). The color of points indicates the logFC values from the Exc LIV-PM DE signature. The colors range from pink (greater expression in LIV samples compared to PM samples) to white (no difference in expression between PM samples and LIV samples) to blue (expression greater in PM samples relative to LIV samples). The colored bar beneath select points in the scatter plot indicates whether the RNA transcript represented by the point is an iEEG Up DEG (green bar) or an iEEG Down DEG (purple bar) for the delta wave DE signature in the Berto et al. study.

in these LIV-PM DE analyses were separate from the 15 LIV samples in the FSCV DE analyses. After multiple test correction, for all 9 of the high-confidence FSCV DE signatures a significant correlation was observed between the FSCV DE signature and the snRNA-seq LIV-PM DE signature in the corresponding cell type, and for 8 of these 9 FSCV DE signatures the direction of the correlation between the FSCV DE signature and the corresponding LIV-PM DE signature showed that the genes associated with greater FSCV metrics were overlapping with genes more highly expressed in LIV samples compared to PM samples. The strongest correlations were the dopamine FSCV DE signatures in PFC neurons (Spearman's $\rho = -0.44$ for Inh and -0.42 for Exc; adjusted p-values $< 2.2 \times 10^{-16}$; Fig. 3). These observations suggest that the high-confidence FSCV DE signatures capture core components of the living human PFC transcriptome.

Replication of FSCV DE signatures in other neurotransmission DE analyses

Given the lack of power in the FSCV DE analyses (i.e., the lack of DEGs when using adjusted p-values to define DEGs), it was important to confirm using independent data that the high-confidence FSCV DE signatures truly reflect a transcriptional signature associated with neurotransmission in the human brain. Towards this end, neurotransmission DE analyses from two independent datasets were utilized.

The first independent dataset was from the DBS surgeries where bulk RNA-seq had been performed on the PFC biopsy obtained during the surgery and MERs (i.e., a technology for measuring neurotransmission intracranially that is distinct from FSCV) were obtained for analysis along white matter tracts

between the PFC biopsy site and the anatomical target for DBS (i.e., subthalamic nucleus [STN] or globus pallidus internus [GPi]) approximately 10 min following the PFC biopsy (Fig. 1). These deep brain targets are known to have direct and indirect anatomical connections to the PFC [35, 36]. From the MER data, neurotransmission was represented quantitatively as the aperiodic exponent, which is a metric derived from local field potentials that captures the balance between neuronal inhibition (larger aperiodic exponent values) and excitation (smaller aperiodic exponent values) in the brain tissue surrounding the microelectrode [37]. MERs were analyzed from 115 DBS surgeries (72 surgeries where the STN was the DBS target and 43 surgeries where the GPi was the DBS target) where bulk RNA-seq from the PFC biopsy obtained during the surgery was available for analysis. For each DBS target, DE was performed between the MER metric and mature RNA transcript expression in the PFC (the full MER DE signatures are in Supplementary Table 3). When using adjusted p-values to define MER DEGs, none were identified, but using the π_1 statistic [33] it was estimated that with larger samples sizes MER DEGs would be identified for both the STN ($\pi_1 = 0.30$) and the GPi ($\pi_1 = 0.29$) MER DE signatures. Comparing each of these two MER DE signatures to each of the 9 high-confidence FSCV DE signatures using Spearman's correlation revealed a significant correlation after multiple test correction for 78% of the comparisons (i.e., 14 of the 18 comparisons between one of the 9 FSCV DE signatures and one of the two MER DE signatures). The strongest correlation was observed between the dopamine Exc FSCV DE signature and the STN MER DE signature (Spearman's $\rho = 0.30$; adjusted p-value = 1.85×10^{-233}; Fig. 3).

The second independent dataset analyzed to assess whether the FSCV DE signatures truly capture information about a transcriptional signature associated with neurotransmission in the human brain was from a previously published study by Berto et al. of 16 individuals undergoing temporal cortex resection to treat epilepsy [19]. The Berto et al. study was of the following design: (1) iEEG recordings (i.e., a technology for measuring neurotransmission intracranially that is distinct from both FSCV and MER) were made of the temporal cortex while participants successfully encoded memories, and from each iEEG recording a metric was derived summarizing each of six frequencies of neural oscillations (alpha, beta, delta, gamma, high gamma, and theta); (2) days after the iEEG recordings, temporal cortex tissue was resected for therapeutic purposes during a neurosurgical procedure; (3) RNA sequencing of the resected temporal cortex tissue was performed; (4) DE was performed for each of the six frequencies of neural oscillations derived from the iEEG recordings. The six lists of iEEG DEGs reported in this published study were downloaded, and each list was split into two lists – one for iEEG Up DEGs and one for iEEG Down DEGs. For each of the 9 high-confidence FSCV DE signatures analyzed, the FSCV Up DEGs and the FSCV Down DEGs were tested for enrichment of the 12 iEEG DEG lists (for a total of 216 tests). After accounting for multiple tests, 10 comparisons survived correction. The most significant enrichment was between the dopamine Exc FSCV Up DEGs and the delta wave iEEG Down DEGs (Fisher's test OR = 6.30, adjusted p-value = 4.11×10^{-45}). A significant enrichment was also seen for dopamine Exc FSCV Down DEGs and the delta wave iEEG Up DEGs (Fisher's test OR = 3.50, adjusted p-value = 2.31×10^{-15}) (Fig. 3).

Identifying TPAWN

Given the different designs of the studies that identified the FSCV, MER, and iEEG DE signatures, the findings presented thus far suggest the coordinated expression of a set of genes may be associated with neurotransmission in the human brain. To identify the set of genes, the following procedure was performed, with input to the procedure being the 9 high-confidence FSCV DE signatures, the two MER DE signatures, and the six iEEG DE signatures: (1) the DEGs for every DE signature were compared to the DEGs of every other DE signature using Fisher's exact tests; (2) two DE signatures were defined as "connected" to one another if a Fisher's exact test comparing the DEGs of the two signatures was significant after multiple test correction; (3) a network was constructed where network nodes were DE signatures and network edges were defined by the previous step; (4) a fully connected sub-component of the network containing at least one DE signature from each of the three types of neurotransmission DE analyses (i.e., FSCV, MER, and iEEG) was identified; (5) genes that were DEGs in DE signatures from at least two of the three types of neurotransmission DE analyses in the fully connected subcomponent were identified. This procedure output a set of 588 genes suspected to be involved in what will be referred to in the remainder of this report as the "transcriptional program associated with neurotransmission" (TPAWN; Supplementary Table 4). For validation purposes, TPAWN genes were compared to genes implicated in neurotransmission through experiments of model systems, and found to be enriched with genes associated to neurotransmission by (1) the NeuroExpresso/NeuroElectro study [38] (OR = 2.88, p-value = 1.53×10^{-8}) and (2) a report on data from the Allen Institute for Brain Science [39] (OR = 1.80, p-value = 2.19×10^{-12}).

TPAWN genes are evolutionarily constrained and linked to brain illness

To further validate the notion that TPAWN genes (i.e. the genes encoding the RNA transcripts in TPAWN) play a key role in neurotransmission and brain function, analyses were performed using data from population genetic studies. First, the evolutionary constraint of TPAWN genes was examined, as more constrained genes have been shown to be enriched for genes implicated in disorders of brain function [40]. Relative to all genes expressed in the brain, TPAWN genes were evolutionarily constrained as measured by having lower "loss-of-function observed/expected upper bound fraction" (LOEUF) scores (K-S test p-value < 2×10^{-16}; Supplementary Figure 3). Second, whole-exome sequencing data from 29,064 ancestrally diverse individuals in a general health system population in New York City was mined to investigate the consequences of rare protein-truncating variants (PTVs) in TPAWN genes on brain functions. This was done by performing a mental health phenome-wide association study on rare PTV carrier status. After multiple test correction for the number of mental health phecodes examined, a significant increase in risk for 'hallucinations' (phecode 292.6) was observed in carriers of rare PTVs in TPAWN genes compared to non-carriers (OR = 3.81, unadjusted p-value = 5.62×10^{-4}, adjusted p-value = 0.04).

TPAWN captures information flow between PFC and deep brain structures

The FSCV and MER DE analyses that led to the identification of TPAWN both involved RNA-seq of PFC samples and intracranial recordings of deep brain structures (i.e., SNr, STN, GPi), suggesting that TPAWN may capture molecular processes occurring within PFC excitatory neurons that communicate molecular information to deep brain structures through axonal projections. To test this hypothesis, a series of analyses were performed on the Exc snRNA-seq data from LIV samples (N = 31 samples; includes the 15 samples in the FSCV DE analyses). For each Exc nucleus, a score was created that captured the activity of TPAWN genes in that nucleus (where higher scores reflected higher expression levels for TPAWN genes). Visualizing the resulting scores, a bimodal distribution was observed (Fig. 4A). In a recent study, Lui et al. characterized seven subtypes of PFC excitatory neurons in rodents and annotated these subtypes with respect to their axonal long-range projections throughout the brain [41]. A score for each of the 7 subtypes was calculated for the Exc cells in the LBP snRNA-seq data, and the association between the TPAWN scores and these 7 subtype scores was assessed using a linear

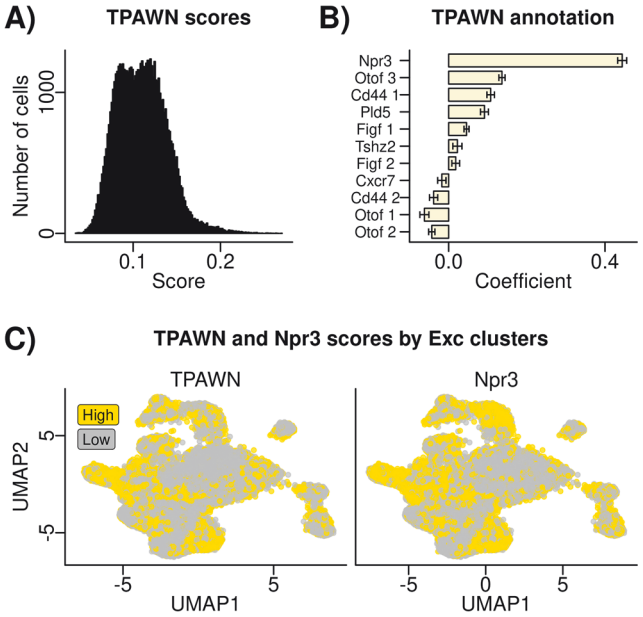

Fig. 4 Transcriptional Program Associated with Neurotransmission (TPAWN). (**A**) TPAWN scores. Histogram showing the distribution of TPAWN scores (x-axis) in 60,084 Exc nuclei from 31 LIV samples with snRNA-seq data. (**B**) TPAWN annotation. Results of linear regression testing the association between TPAWN scores (dependent variable) and scores reflecting the activity of genes reported by Lui et al. to be markers of PFC excitatory neuron projection patterns in mice. The y-axis indicates the different types of PFC projection excitatory neurons in mice using the marker naming scheme in Lui et al.. The x-axis is the beta coefficient between the signature indicated on the y-axis and the TPAWN scores from the linear model. Error bars indicate the 95% confidence interval. (**C**) TPAWN and Npr3 scores by Exc clusters. Scatter plot showing the clustering of 60,084 Exc nuclei from 31 LIV cells. The gene expression data from these cells was reduced to two dimensions using the UMAP approach (shown on the x-axis and y-axis). In the left plot, the points are colored by whether the TPAWN score in the nucleus was high or low. In the right plot, the points are colored by whether the Npr3 score in the nucleus was high or low. For both plots, the categorization of a nucleus as high or low was done based on whether its score was greater than or less than the mean. FSCV – fast scan cyclic voltammetry; DE – differential expression; DA – dopamine; ST – serotonin; NE – norepinephrine; Exc – excitatory neurons; Inh – inhibitory neurons; Ast – astrocytes; OPC – oligodendrocyte progenitor cells; Micro – microglia; Oli – oligodendrocytes; TPAWN – transcriptional program associated with neurotransmission; MER – microelectrode recording; iEEG – intracranial electroencephalography.

model that included all 7 subtype scores as independent variables. This analysis found the subtype labeled Npr3 in Lui et al. had the strongest association to TPAWN scores, with the regression model coefficient for this variable over 3.5-fold the magnitude of the regression model coefficient for the next strongest associated variable (Fig. 4B; Supplementary Figure 4). Exc with high TPAWN and Npr3 scores were not isolated in a single subcluster of Exc cells in UMAP space (Fig. 4C). Lui et al. determined that Npr3 cells were preferentially located in layer 5 of the rodent PFC and had projections to many of the rodent deep brain structures examined in their study. Based on these observations, TPAWN in the human PFC identified with the FSCV and MER DE analyses may be driven by subcortical-projecting excitatory neurons.

DISCUSSION

The main objective of the LBP study reported here was to determine if there is a reproducible gene expression signature associated with measures of neurotransmission obtained from the brain of living humans. To do this, gene expression was characterized in 130 PFC samples obtained during neurosurgical procedures from participants of the LBP moments before neurotransmission was measured intracranially, in some cases while the participant played a computer game engaging brain functions. Through the FSCV DE analyses, gene expression signatures within multiple PFC cell types were linked to fluctuations of dopaminergic, serotonergic, and noradrenergic neurotransmission in the substantia nigra in response to monetary offers made to participants by a computer avatar. These signatures were reproduced in the MER and iEEG DE analyses, and the three types of neurotransmission DE signatures were integrated to prioritize a set of genes (i.e., TPAWN) for further study based on having support in multiple types of neurotransmission DE signatures. TPAWN was validated through analyses of data from published rodent and cell line experiments investigating the relationship between measures of neurotransmission and gene expression. TPAWN genes were found to be more evolutionarily constrained than other genes expressed in the brain, and evidence was found that loss-of-function variants in TPAWN genes may have brain health consequences. In PFC excitatory neurons of LBP participants, higher expression of TPAWN genes tracked with higher expression of genes that in rodent PFC samples are markers of a class of excitatory neurons that connect the PFC to deep brain structures.

Proteins are the ultimate effectors of neurotransmission and brain functions, yet gene expression is the focus of this report. By and large, it is for technical reasons that the transcriptome is the focus rather than the proteome – methods have been developed to enable routine measurement of expression levels of thousands of individual transcripts in thousands of individual nuclei in a single tissue sample, whereas no such robust methods yet exist for measuring the expression levels of proteins. Focusing on gene expression places at the center of this report an assumption that there is a transcriptional signature at the foundation of neurotransmission in the human brain. Current understanding of RNA and protein biology suggests this should be the case – the half-life of RNA in the cell is generally on the order of hours, and the transcriptome provides cells with the ability to respond with agility to changing environmental conditions [42]. Moreover, the transcriptome is a defining feature of tissue type, suggesting there should be aspects of the brain transcriptome that capture the brain's basic functionality (i.e., neurotransmission). The first study to perform neurotransmission DE by pairing RNA sequencing of human brain tissue samples with intracranial neurotransmission recordings from the same individuals was the study by Berto et al. that identified the iEEG DE signatures used in this report [19]. By applying a similar study design to two LBP cohorts, the current study integrated three different types of neurotransmission DE signatures (i.e., FSCV DE signatures; MER DE signatures; iEEG DE signatures) derived from a total 146 neurosurgical procedures (FSCV DE analyses $N = 15$, MER DE analyses $N = 115$; iEEG DE analyses $N = 16$) to identify TPAWN. While the three types of neurotransmission DE analyses were of the same general experimental design (i.e., pairing RNA sequencing of brain tissue samples with intracranial neurotransmission recordings from the same individuals), the experimental designs also differed from one another in nine key ways.

First, each type of neurotransmission DE analysis used a different intracranial recording technology (i.e., FSCV, MER, or iEEG). Second, for FSCV DE analyses, the RNA sequencing technology utilized was snRNA-seq, whereas for the MER and iEEG DE analyses the RNA sequencing technology utilized was bulk RNA-seq. Third, for iEEG DE analyses, the brain region recorded and the brain region sampled were the same (i.e., the MTG), whereas for the FSCV and MER DE analyses the brain region recorded (for FSCV DE analyses, the SNr; for MER DE analyses, the

STN and GPi) differed from the brain region sampled (i.e., the PFC). Fourth, the brain region sampled for the iEEG DE analyses differed from the brain region sampled for the FSCV and MER DE analyses. Fifth, different brain regions were recorded for each type of neurotransmission DE analysis. Sixth, the timing of the brain recording and sampling relative to one another for the FSCV and MER DE analyses (i.e., biopsy followed 10 min later by recording) differed from the timing of the brain recording and sampling relative to one another for the iEEG DE analyses (i.e., recording followed days later by biopsy). Seventh, different metrics were used to represent neurotransmission for each of the three types of neurotransmission DE analyses (i.e., for FSCV DE analyses, the neurotransmitter association with offer size; for MER DE analyses, the aperiodic exponent; for iEEG DE analyses, waveforms). Eighth, for the FSCV and iEEG DE analyses, study participants engaged in tasks that engaged brain function during the recordings, whereas for the MER DE analyses study participants were at rest during the recordings. Ninth, for the FSCV and MER DE analyses the study participants were individuals undergoing DBS electrode implantation to treat PD and other conditions that are indications for DBS, whereas for the iEEG DE analyses the study participants were individuals undergoing surgery to treat epilepsy.

These nine key differences in experimental design are simultaneously a strength and a limitation of this study. On the one hand, the convergence of the neurotransmission DE signatures on TPAWN despite these experimental design differences speaks to the robustness and generalizability of the signal. On the other hand, these experimental design differences render interpretation of the results difficult (e.g., the meaning of the direction of logFC values across the different types of neurotransmission DE analyses is not intuitive). The study had several additional noteworthy limitations. Perhaps most importantly, at the current sample sizes few DEGs were identified using adjusted p-values, and as a result unadjusted p-values were used to define DEGs (in conjunction with orthogonal validation) for the purposes of downstream analyses. This general practice – using unadjusted p-value thresholds to link a molecular signature (e.g., a set of genes) to a trait in a context where the statistical power to link any single molecule (e.g., a single gene) to the trait is inherently limited – has established precedent in bioinformatics (e.g., the calculation of a polygenic risk score) [43]. In this report, applying the strategy amounted to accepting Type I errors when defining individual gene-trait associations in order to avoid Type II errors when identifying transcriptome-wide signatures of traits. Other noteworthy limitations of the study included: performance on the ultimatum game task could be confounded by a variety of factors (e.g., individual differences in the perception of monetary rewards); the extent to which TPAWN generalizes to other cognitive tasks or resting-state conditions could not be comprehensively assessed; it was not possible to confidently address whether cell subtypes (e.g., subtypes of excitatory neurons) are driving particular findings; the study did not address whether distinct neural circuits have unique transcriptomic foundations; while neurons are the cell type most directly involved in neurotransmission, this study found neurotransmission DE signal in the transcriptome of all brain cell types but could not dissect how the transcriptome of different cell types contribute to neurotransmission. To address these and other limitations, future larger studies of neurosurgical cohorts should aim to systematically pair molecular measurements from across the brain to neurotransmission measurements from across the brain to gain a deeper understanding of the observations made here. Such knowledge will facilitate the development of therapeutics that target neural circuit activities in a precise manner to treat brain illnesses.

As noted at the outset of this report, an aim of brain research is to advance knowledge of how brain functions emerge from brain tissue in humans. Tools available to researchers who study the brain in humans to achieve this aim include tools for assessing brain functions (e.g., the ultimatum game), tools for recording brain activity (e.g., intracranial recordings), and tools for characterizing brain biology (e.g., RNA sequencing). Most applications of the tools available for characterizing human brain biology have been applied to samples obtained from individuals in the postmortem setting, when neurotransmission and brain function have ceased. As a result, the molecular foundations of human brain function are not being adequately studied. The current report (including further discussion in the Supplementary Information) provides one approach to bridge this gap and illustrates how the scope of neuroscience can be broadened by studying biology in brain tissue obtained during neurosurgical procedures in conjunction with research activities that use tools for assessing brain functions and for recording brain activity.

METHODS

Ethics statement

All human subjects research for the LBP was carried out in accordance with the relevant guidelines and regulations under STUDY-13-00415 of the Institutional Review Board (IRB) of the Human Research Protection Program at the Icahn School of Medicine at Mount Sinai. Research participants in the living cohort provided informed consent for sample collection, genomic profiling, clinical data extraction from medical records (including microelectrode recording data), and public sharing of de-identified data. A subset of the participants in the living cohort additionally consented to the FSCV recording component of the study, which consisted of FSCV recordings and the ultimatum game. The LBP has undergone annual continuing review by the IRB since the LBP enrollment began in 2013, and in this time, the IRB has never highlighted any major concerns about the enrollment and consent procedures for the study. In addition to the annual IRB review, the LBP Data Safety Monitoring Board comprised of experts not involved in the LBP has met annually since LBP enrollment began in 2013 and has had no concerns about the enrollment and consent procedures for the study. A division of the New York State Department of Health conducted a review of the Living Brain Project from June 17th, 2024, to June 18th, 2024, and issued no findings related to the conduct of the Program.

Living brain project cohort

All of the individuals and PFC samples studied in the current report were first introduced in earlier LBP reports [14]. In the methods sections of those reports can be found descriptions of the living cohort, the postmortem cohort, PFC sample collection procedures, and clinical data collection.

Fast-scan cyclic voltammetry (FSCV) recordings

FSCV recordings were made during 15 DBS surgeries. The procedures used for making the FSCV recordings are fully described in Batten et al. [17] and summarized in this section.

Experimental setup. FSCV recordings were made while study participants played 60 rounds of the ultimatum game [29, 30]. For 6 of the 9 participants in this component of the LBP, the ultimatum game was performed twice (i.e., in separate DBS surgeries) and for 3 participants it was performed once. Participants performed a short practice session both before and within a DBS surgery. During DBS surgery, study participants laid in a semi-upright condition and viewed a task presentation monitor at a distance of around 100 centimeters. They used a gamepad to submit their responses to the trial offers. The FSCV recordings were obtained approximately 10 min after PFC biopsies.

Description of the ultimatum game. In each round of the ultimatum game, the participant must decide whether to accept or reject a monetary offer made by an avatar (the "proposer"). The proposer offers a split of $20 to the participant, and the offer is allowed to range from $1 to $9. If the study participant accepts the offer, they get the offered amount and the proposer gets the remaining amount (i.e., the difference between $20 and the offer). If the participant rejects the offer, neither the participant nor the proposer receives any money.

FSCV recording technology. Approximately 10 min after PFC biopsy, electrochemical recordings were made from the substantia nigra pars reticulata (SNr) using a custom-made carbon-fiber (CF) electrode [26]. From these recordings, the estimates of dopamine, serotonin, and norepinephrine fluctuations were made using deep convolutional neural networks that were trained and tested on in vitro data that consisted of 64 datasets collected by exposing 64 CF electrodes to varying concentrations of dopamine, serotonin and norepinephrine in a saline solution [17, 44].

Deriving FSCV metrics used in differential expression analyses. For each neurotransmitter, activity during a proposed offer period was measured as the area under the curve (AUC) of the neurotransmitter measurements made during the offer period. The offer period was defined as the one second following the moment the offer was first shown to the subject. Neurotransmitter measurements were made at 10 points during this period spaced 0.1 s apart, and the AUC value was calculated as the sum of these measurements. The measurement at time 0 was subtracted out of each measurement before the sum was calculated. Since 60 offers were made during the game, 60 AUC values for each neurotransmitter resulted from this process. Both the AUC values and offer amounts were then transformed into z-scores, which were then input into a linear regression model using the following formula to calculate beta coefficients between neurotransmitter AUC values and offer amount values. These analyses were performed using the Statistics Toolbox in MATLAB R2023a.

Formula 1 (linear model with fixed effects):

$$Neurotransmitter\ AUC \sim Offer\ amount + Residuals$$

Single-nucleus RNA sequencing (snRNA-seq)

The methods used to perform RNA extraction, RNA sequencing, and initial data quality control for the LBP snRNA-seq dataset analyzed in the current report are introduced and fully described in Vornholt et al. [21]. The output of these initial quality control procedures was 362,310 nuclei from 31 LIV samples and 21 PM samples.

Background-corrected UMI matrices from the samples that remained after sample filtering were then merged together into a single matrix including 362,310 nuclei from 52 samples (31 LIV samples and 21 PM samples). These counts were normalized to counts-per-million (CPM) using the RelativeCounts() function of the Seurat R package with a scale factor of 10^6. A value of 1 was added to each value in the CPM matrix, and these values were then log2-normalized using the log2() function of the base stats R package. The 2,000 most highly variable genes were identified in the log2-normalized matrix using the FindVariableFeatures() function of the Seurat R package with the "selection.method" parameter set to "vst." The log2-normalized counts for these 2,000 genes were then adjusted to account for the unwanted effects of technical variables (i.e., number of counts, number of genes, percentage of counts mapping to exons) on gene expression using the ScaleData() function of the Seurat R package. Principal components analysis was performed on the adjusted log2-normalized counts using the RunPCA() function of the Seurat R package. The effects of sample identity on the top 15 principal components was accounted for by adjusting the top 15 principal components using the RunHarmony() function of the harmony R package (version 1.1). The harmony-adjusted principal components were then input into the FindNeighbors() and FindClusters() functions of the Seurat R package to identify clusters of nuclei, with the "resolution" parameter of the FindClusters() function set to 0.6.

Cell clusters were then annotated into 6 broad classes: excitatory neurons [Exc]; inhibitory neurons [Inh]; oligodendrocytes [Oli]; astrocytes [Ast]; microglia [Micro]; oligodendrocyte progenitor cells [OPCs]. Annotations were made by comparing clusters to clusters of the same nuclei previously annotated in the Vornholt et al report [21]. The clustering solution for this report differs slightly from the clustering solution in Vornholt et al. because in this report the effect of technical variables were regressed out prior to clustering.

Differential expression analyses performed using the snRNA-seq data utilized "pseudo-bulk" counts. For each cell type studied (i.e., Exc, Inh, Oli, Ast, Micro, OPC), a pseudo-bulk count matrix was calculated using aggregateData() function of the muscat R package (v1.10.1) that had one column for every sample and one row for every gene detected in the nuclei annotated to that cell type. The values in these matrices were the sum of the background-corrected UMI counts for the gene in the nuclei from the sample annotated to the cell type.

Microelectrode recordings (MERs)

Intracranial MERs are routinely obtained for clinical purposes from awake patients during DBS surgery to pinpoint where to place the DBS electrode. For this report, MERs were analyzed from a subset of the DBS surgeries where bulk RNA-seq had been performed on the PFC biopsy obtained during the surgery. MERs were obtained approximately 10 min following PFC biopsies using the Guideline 4000 (FHC, Inc. Bowdoin, ME) and a tungsten monopolar microelectrode (22675Z, FHC, Inc. Bowdoin, ME) with a 44000 Hertz (Hz) sampling frequency and analyzed offline.

MERs were retained for analysis if (1) the MER was taken in the STN or GPi, as determined by the distance between the microelectrode and the target (STN: 0–5 mm, GPi: 0–6 mm); (2) the duration of the MER was at least 5 s. To exclude artifacts and the need to include an 'aperiodic knee' in subsequent analysis steps, a finite input response bandpass filter of 2–50 Hz was applied to the local field potential (LFP) time series data derived from the MERs using the filter_signal() function within the NeuroDSP Python package (v2.2.1). The output of this filter was then down sampled to 1000 Hz using the signal.resample() within the Scipy Python package (v1.12.0). Power spectrum densities (PSD) within the frequency range of 2–50 Hz were then calculated with the Welch method for each MER using the compute_spectrum() function within the NeuroDSP Python package.

Spectral parameterization was then applied to extract timescales from PSDs using the FOOOF() function from the FOOOF Python package (v1.1.0) [45], which decomposes log-power spectra into periodic components and the aperiodic exponent. Periodic components are modeled as Gaussians, and the aperiodic exponent is modeled as a generalized Lorentzian function centered at 0 Hz. This approach is preferred for analyzing neural signals wherein a strong 1/f power law is present. This allows for oscillatory, or periodic, components to be easily accounted for and ignored in the frequency domain when inferring the aperiodic exponent of the PSD [45]. Each PSD was fit across the FOOOF algorithm with settings (peak_width_limits = [2,7], max_n_peaks = 3, min_peak_height = 0.05, peak_threshold = 2, aperiodic_mode = 'fixed') across the frequency range 5–45 Hz. This provided an aperiodic exponent value that reveals baseline power across frequencies (1/f), reflecting the balance of neuronal excitation and inhibition within each LFP time series. Recordings with a FOOOF model fit of $R^2 < 0.8$ and aperiodic exponent < 0 were excluded from analyses to avoid the use of data from poor quality recordings.

Bulk RNA-seq

The methods used to perform RNA extraction, RNA sequencing, cell type deconvolution, and data quality control for the bulk RNA-seq data analyzed in the current report are introduced and fully described in Liharska et al., *including* the methods used to identify confounders to account for in the bulk RNA-seq data analyzed in the current report [14]. Levels of the mature forms of each RNA transcript detected in the bulk RNA-seq data were quantified as described in Kopell et al [15].

Identity concordance

To identify sample mislabeling events, identity concordance between samples was performed using genetic variants called from all sequencing data available from the LBP (includes the data analyzed in the current report and additional types of sequencing data featured in other LBP reports). More than one data source was available for identity concordance for all but one individual ever sequenced for LBP. Variants were called from RNA sequencing data following Genome Analysis Toolkit (GATK) best practices. The approach used to determine if two variant call sets were from the same individual differed depending on the sources of the call sets in the comparison (e.g., RNA sequencing data to RNA sequencing data, WGS to RNA sequencing data). For comparisons of (1) two call sets from bulk RNA sequencing data, (2) two callsets from single-cell RNA sequencing data, and (3) two call sets from WGS data, gtcheck from the bcftools software package (v1.9) was used to calculate the percentage of sites concordant between the call sets. For comparisons of (1) bulk RNA sequencing data call sets to single-cell RNA sequencing data call sets, (2) WGS data callsets to bulk RNA sequencing data call sets, and (3) WGS data callsets to single-cell RNA sequencing data call sets, genotyping matrices were read into R, discrepancies between allele code fields were corrected, sites covered in only one call set were removed, and Pearson's correlations of genotype similarity were calculated for every pair of call sets. Regardless of the approach used to calculate concordance between call sets, a threshold for deciding whether two samples came from the same individual was determined manually by assessing the distribution of

similarity metrics. Mismatches were defined as (1) instances where two samples expected to be from the same individual were genetically discordant and (2) instances where two samples not expected to be from the same individual were genetically concordant. All mismatches identified by the thresholding procedure were further examined to confirm a true mismatch (i.e., using all RNA sequencing data and WGS data call sets from the individuals in the mismatch).

FSCV DE analyses

Each of the pseudo-bulk count matrices was filtered to retain the 15 LIV samples with FSCV recordings. Lowly expressed genes were then removed from each matrix using the default settings of the filterByExpr() function in the edgeR R package (v3.38.1). The pseudo-bulk counts of remaining genes were normalized using the voomWithDreamWeights() function of the dream software within the variancePartition R package. A total of 18 FSCV DE analyses were performed (one in each of the six cell types for each of the three neurotransmitters [dopamine, serotonin, norepinephrine]). For each of these 18 FSCV DE analyses, DE was run on the voom-normalized pseudo-bulk count matrix using the dream() function in the variancePartition R package and the formula indicated below. For all FSCV DE analyses, multiple test correction was done using an FDR of 5%. FSCV DEGs were defined using an unadjusted p-value threshold of 0.05. FSCV DE signature π_1 statistics [33] were estimated using the qvalue R package (v2.28.0). KEGG enrichment of FSCV DEGs was performed as described below.

Formula 2 (linear model with fixed effects and random effects for individual ID and and sex):

$$\textit{RNA Transcript Expression} \sim \textit{FSCV Metric} + \textit{Individual ID} + \textit{Sex} + \textit{Number of Nuclei} + \textit{Mean Reads Per Nucleus} + \textit{Fraction of Reads in Nuclei} + \textit{Residuals}$$

KEGG enrichment tests

Gene set enrichment analyses were performed using the Kyoto Encyclopedia of Genes and Genomes (KEGG) database [34]. The htext-formatted hsa00001 KEGG database was downloaded on October 4th, 2021, via the KEGG web server and parsed into structured data tables in python. The output of this script was a row for every instance of a gene's membership in a KEGG gene set and one column each for gene symbol, gene set ("KO reference pathway"), parent category of the gene set ("super pathway"), and the broad concept grouping of the parent category ("top-level string"). Gene symbols provided by KEGG were mapped to Ensembl identifiers with a mapping file generated using the HUGO [46] web server on June 10th, 2020. All KEGG gene sets with the top-level string "Human" were excluded from analysis since these gene sets may be derived from studies of postmortem human tissues. Sets with less than 10 member genes were excluded from analysis, leaving 278 KEGG gene sets tested for enrichment. These 278 KEGG gene sets were tested for enrichment of DEGs in R using the fisher.test() function in the base stats package as the overlap between the genes in the KEGG gene set and DEGs, using as background the set of genes (i.e., RNA transcripts) in the DE analysis. KEGG gene sets with statistically significant associations were mapped to parent terms via the source data file. Multiple testing correction was carried out separately for each of the DE signatures investigated accounting for the 278 KEGG gene sets tested using the false discovery rate estimation method of Benjamini and Hochberg [47] implemented in R using the p.adjust() function of the base stats package.

Comparing DE signatures

Spearman's correlations between pairs of DE signatures presented throughout this report were calculated using the cor.test() function in the R base stats package. Multiple test correction for these Spearman's correlations was not performed because the majority of unadjusted p-values returned by the cor.test() function were estimated to be 0 (indicated in the main text using the "p-value $< 2.2 \times 10^{-16}$" notation). When throughout this report the overlap between two DEGsets was compared using Fisher's exact test (e.g., FSCV DEGs and iEEG DEGs), the Fisher's exact test was implemented by the fisher.test() function in the base stats R package.

MER DE analyses

DE of the aperiodic exponent values was performed on the voom-normalized mature RNA transcript bulk RNA-seq data separately for the STN (N = 72 LIV samples from 54 individuals) and GPi (43 LIV samples from 28 individuals) using the dream() function in the variancePartition R package and the formula indicated below. The covariates to include in the formula were selected based on a covariate selection process performed for LIV-PM bulk RNA-seq DE analyses reported in Liharska et al. [14] with the exception that for MER DE the estimated percentage of neuronal cells was not used as a covariate in order to maximize the comparability between the MER DE and the snRNA-seq FSCV DE signatures. For all MER DE analyses, multiple test correction was done using an FDR of 5%. MER DEGs were defined using an unadjusted p-value threshold of 0.05. MER DE signature π_1 statistics [33] were estimated using the qvalue R package (v2.28.0).

Formula 3 (linear model with fixed effects and random effects for individual ID and and sex):

$$\textit{RNA Transcript Expression} \sim \textit{Aperiodic Exponent} + \textit{Individual ID} + \textit{Sex} + \textit{RIN} + \textit{Picard RNASeqMetrics Median 3 Prime Bias} + \textit{Picard RNASeqMetrics PCT mRNA Bases} + \textit{Depletion Batch} + \textit{Picard InsertSizeMetrics Median Insert Size} + \textit{Alignment Summary Metrics} + \textit{Residuals}$$

Intracranial electroencephalography (iEEG) DE analyses

RNA transcript associations with neural oscillations measured using iEEG were obtained from Supplementary Table 2 of the Berto et al. publication (sheet entitled "SME Univariate Stats") [19]. Gene symbols were mapped to ensembl gene identifiers using HUGO. Since the published associations were already limited to genes with significant associations (i.e., IEEG DEGs), no further filtering was done (2,380 unique ensembl gene identifiers).

Identification of TPAWN

To identify the set of RNA transcripts referred to as "TPAWN" in the results, the following procedure was performed. The initial input to the procedure was 17 neurotransmission DE signatures (the 9 FSCV DE signatures with π_1 values greater than 0.10; the two MER DE signatures; and the 6 iEEG DE signatures). Two DEG lists were made from each of the DE signatures: Up DEGs (i.e., DEGs with positive logFC values) and Down DEGs (i.e., DEGs with negative logFC values). As described above, for the FSCV and the MER DE signatures DEGs were defined using unadjusted p-value thresholds and for the iEEG DE signatures DEGs were defined in the Berto et al. publication [19]. Each of the 17 neurotransmission DE signatures was compared to the other 16 neurotransmission DE signatures by performing the following 4 Fisher's exact tests (for a total of 544 tests):

(1) Up DEGs from the first DE signature were compared to Up DEGs in the second signature
(2) Up DEGs from the first DE signature were compared to Down DEGs in the second signature
(3) Down DEGs from the first DE signature were compared to Up DEGs in the second signature
(4) Down DEGs from the first DE signature were compared to Down DEGs in the second signature

For comparisons of two LBP neurotransmission DE signatures, the set of background genes used in the Fisher's exact test was the intersect between the genes present in the two DE signatures. For comparisons between a LBP neurotransmission signature and a iEEG DE signature, the set of background genes used in the Fisher's exact test was the set of genes present in the LBP DE signature. This was necessary because the full DE signature (i.e., logFCs from all genes tested) was only available for LBP neurotransmission DE signatures (i.e., the full iEEG DE signatures were not published, only the iEEG DEGs were published). For comparisons between two iEEG DE signatures, the set of 30,099 RNA transcripts expressed in the bulk RNA-seq mature RNA DE analyses were used as the background. After correcting for 544 tests using the FDR of 5%, any two signatures with at least one significant test with an odds ratio greater than 1 were considered "connected" to one another, resulting in 49 connections between 16 neurotransmission DE signatures. These connections served as the input to construct an undirected graph using the igraph R package (v1.4.1), where nodes were the 16 DE signatures and edges were the 49 connections between these signatures. Fully connected subcomponents of the graph were identified using the maximal.cliques() function of the igraph R package, and the resulting list of subcomponents was filtered to include only those subcomponents that included a node from each of the three

types of neurotransmission DE signatures (i.e., FSCV, MER, and iEEG). Only one such subcomponent was identified. The union of the DEGs from the nodes in this subcomponent was then compiled, and genes that were DEGs in signatures in at least two types of neurotransmission DE (i.e., FSCV and MER; FSCV and iEEG; MER and iEEG) were considered part of the TPAWN (N = 588 RNA transcripts).

Enrichment of TPAWN genes in relevant external data

NeuroExpresso/NeuroElectro data. The NeuroExpresso/NeuroElectro study [38] associated RNA transcripts to neurotransmission by integrating RNA transcript expression data generated using microarray technology from mouse brain tissue with data manually curated from the literature characterizing electrophysiological properties of rodent brain cells. A set of approximately 1,000 RNA transcripts identified by the NeuroExpresso/NeuroElectro study as being significantly associated with an electrophysiological property was downloaded (i.e., the list of RNA transcripts the NeuroExpresso/NeuroElectro study team published in Supplementary Table 3 of the NeuroExpresso/NeuroElectro study report [38]). A Fisher's exact test was performed using the fisher.test() function in the base stats R package to assess the overlap between these RNA transcripts and the RNA transcripts in TPAWN. The background set of genes used in the Fisher's exact test was the 30,099 genes expressed in the PFC in the bulk RNA-seq mature RNA transcript expression data.

Allen institute for brain science data. Published analyses of data from the Allen Institute for Brain Science [39] associating RNA transcript expression to electrophysiological properties were downloaded ("Online Table 1" at https://github.com/PavlidisLab/transcriptomic_correlates). The downloaded table contained all associations between a RNA transcript and a electrophysiological property identified by the authors. The overlap between the set of associated RNA transcripts in the downloaded table and the RNA transcripts in TPAWN was assessed using a Fisher's exact test was performed using the fisher.test() function in the base stats R package. The background set of genes used in the Fisher's exact test was the 30,099 genes expressed in the PFC in the bulk RNA-seq mature RNA transcript expression data.

Evolutionary constraint. Evolutionary constraint of genes was defined using "loss-of-function observed/expected upper bound fraction" (LOEUF) scores from the Genome Aggregation Database (gnomAD) [40]. The distribution of LOEUF scores in genes encoding the 588 RNA transcripts in TPAWN was compared to distribution of LOEUF scores in all other genes expressed in PFC in the bulk RNA-seq mature RNA transcript expression data using the ks.test() function in the base stats R package.

Mental health phenome-wide association study. Genetic and clinical data from the Mount Sinai Million Health Discoveries Program (MSM-HDP; formerly, the BioMe Biobank Program; N = 29,064) were analyzed to test the effects of rare PTVs in the genes encoding RNA transcripts in TPAWN on illnesses of brain functions. The genetic data was comprised of whole-exome sequencing (for identifying rare PTVs) and microarray (for calculating genetic principal components); the clinical data was comprised of billing codes from the electronic medical records that had been mapped to phecodes [48–51]. Variants in the MSM-HDP call set were annotated for their predicted effect on protein function using the Variant Effect Predictor (VEP; v96) software with the LOFTEE plugin. PTVs were defined as any variant annotated by the LOFTEE plugin as "loss-of-function" with either "high confidence" or "low confidence." PTVs were defined as rare if the minor allele count in the MSM-HDP cohort was less than or equal to five. A phenome-wide association study (PheWAS) was run using the phewas() function of the PheWAS() R package (v0.99.5-5) to test the association between each phecode and being a carrier of a rare PTV in one of the genes encoding RNA transcripts in TPAWN. The top 20 genetic principal components were used as covariates. After running the PheWAS, phecodes were grouped into broad categories using the phewasManhattan() function of the PheWAS R package, and the 68 phecodes in the "mental disorders" category were retained for analysis. Multiple test correction for these 68 phecodes was performed using the method of Benjamini and Hochberg implemented in R using the p.adjust() function of the base stats package.

Annotating TPAWN in Exc to Npr3 Exc neurons

A score representing the activity of the 588 RNA transcripts in TPAWN in each nucleus of the snRNA-seq data from LIV samples (N = 31; N = 60,834 nuclei) was calculated using the AUCell_run() function of the AUCell R package (v1.18.1). For visualization of these 60,834 nuclei in UMAP dimensions, the same procedure was followed that was described above for the full set of 362,310 nuclei. The mean TPAWN score amongst these 60,834 nuclei was calculated. Nuclei with scores greater than the mean were labeled as having high TPAWN scores and nuclei with scores lower than the mean were labeled as having low TPAWN scores. The 60,834 Exc nuclei were annotated with respect to transcriptional signature of mouse PFC excitatory neurons with known axonal projection patterns. These signatures were downloaded from a published study [41], and a score for each signature was calculated using the AUCell_run() function of the AUCell R package (v1.18.1). The relationship between the mouse PFC projection neuron scores and the TPAWN scores was assessed using linear regression implemented with the lm() function of the base stats R package. The TPAWN score was the dependent variable in the linear regression model and the mouse PFC projection neuron scores were the dependent variables. To visualize TPAWN scores against Npr3 scores, a score for the Npr3 signature was re-calculated using the AUCell_run() function of the AUCell R package (v1.18.1) after removing genes from the Npr3 signature that were also in TPAWN.

LIV-PM DE in sn-RNAseq data

LIV-PM DE in the snRNA-seq data was performed for each cell type in order to compare FSCV DE signatures to a LIV-PM DE signature of the same cell type from an independent set of samples. Three filters were applied to each pseudo-bulk count matrix (31 LIV samples and 21 PM samples) to create the datasets for LIV-PM DE: (1) the 15 LIV samples in the FSCV DE analyses were removed; (2) one of the PM samples that was a technical replicate of another PM sample was removed; (3) for living participants with two LIV samples, one sample was removed. These filters resulted in 13 LIV samples and 20 PM samples (one sample per individual) for analysis. Lowly expressed genes were then removed from the pseudo-bulk counts matrices using the default settings of the filterByExpr() function in the edgeR R package (v3.38.1). Since these matrices consisted of one sample per individual, the pseudo-bulk counts of expressed genes were normalized using the voom() function of the limma R package (v3.46.0) [52] and DE of LIV-PM status was performed using the lmFit() function of the limma R package using the following formula (determined as described in Vornholt et al. [21]):

Formula 4 (linear model with fixed effects and random effects for individual ID and sex):

$$\textit{RNA Transcript Expression} \sim \textit{LIV} - \textit{PM Status} + \textit{Individual ID} + \textit{Sex} + \textit{Number of Nuclei} + \textit{Mean Reads Per Nucleus} + \textit{Fraction of Reads in Nuclei} + \textit{Residuals}$$

DATA AVAILABILITY

All data analyzed from the full LBP cohort are available via the AD Knowledge Portal (https://adknowledgeportal.org). The AD Knowledge Portal is a platform for accessing data, analyses, and tools generated by the Accelerating Medicines Partnership (AMP-AD) Target Discovery Program and other National Institute on Aging (NIA)-supported programs to enable open-science practices and accelerate translational learning. The data, analyses and tools are shared early in the research cycle without a publication embargo on secondary use. Data is available for general research use according to the following requirements for data access and data attribution (https://adknowledgeportal.org/DataAccess/Instructions). For access to content described in this manuscript see: https://www.synapse.org/#!Synapse:syn51622714/datasets/

REFERENCES

1. Alberts B. *Molecular biology of the cell*. Seventh edition. edn, (W. W. Norton & Company; New York; 2022).
2. Schadt, EE, Monks, SA, Drake, TA, Lusis, AJ & Che, N in *Nature* 2003.
3. Kavalali ET. The mechanisms and functions of spontaneous neurotransmitter release. Nat Rev Neurosci. 2015;16:5–16. https://doi.org/10.1038/nrn3875
4. Kozlov, M Famous 'homunculus' brain map redrawn to include complex movements. Nature 2023. https://doi.org/10.1038/d41586-023-01312-6
5. Penfield W, Rasmussen T. *The Cerebral Cortex of Man*. (Macmillan; New York; 1950).
6. Wang D, Liu S, Warrell J, Won H, Shi X, Navarro FCP, et al. Comprehensive functional genomic resource and integrative model for the human brain. Science. 2018;362:eaat8464 https://doi.org/10.1126/science.aat8464

7. Hodes RJ, Buckholtz N. Accelerating Medicines Partnership: Alzheimer's Disease (AMP-AD) Knowledge Portal Aids Alzheimer's Drug Discovery through Open Data Sharing. Expert Opin Ther Targets. 2016;20:389–91. https://doi.org/10.1517/14728222.2016.1135132
8. Fromer M, Roussos P, Sieberts SK, Johnson JS, Kavanagh DH, Perumal TM, et al. Gene expression elucidates functional impact of polygenic risk for schizophrenia. Nat Neurosci. 2016;19:1442–53. https://doi.org/10.1038/nn.4399
9. De Jager PL, Ma Y, McCabe C, Xu J, Vardarajan BN, Felsky D, et al. A multi-omic atlas of the human frontal cortex for aging and Alzheimer's disease research. Sci Data. 2018;5:180142 https://doi.org/10.1038/sdata.2018.142
10. Beckmann ND, Lin WJ, Wang M, Cohain AT, Charney AW, Wang P, et al. Multiscale causal networks identify VGF as a key regulator of Alzheimer's disease. Nat Commun. 2020;11:3942 https://doi.org/10.1038/s41467-020-17405-z
11. Ament SA, Adkins RS, Carter R, Chrysostomou E, Colantuoni C, Crabtree J, et al. The Neuroscience Multi-Omic Archive: a BRAIN Initiative resource for single-cell transcriptomic and epigenomic data from the mammalian brain. Nucleic Acids Res. 2023;51:D1075–D1085. https://doi.org/10.1093/nar/gkac962
12. Sarbey B. Definitions of death: brain death and what matters in a person. J Law Biosci. 2016;3:743–52. https://doi.org/10.1093/jlb/lsw054
13. Akkus, S, Simons, NW, Mahtani, S, Epstein, E, Zuccaro, P, Hashemi, A et al. Safety of prefrontal cortex biopsies during deep brain stimulation procedures. Neurosurgery, (9900). https://doi.org/10.1227/neu.0000000000003711
14. Liharska, LE, Park, YJ, Ziafat, K, Wilkins, L, Silk, H, Linares, LM et al. A study of gene expression in the living human brain. Mol Psychiatry 2025. https://doi.org/10.1038/s41380-025-03163-1
15. Kopell BH, Kaji DA, Liharska LE, Vornholt E, Lund A, Hashemi A, et al. A study of RNA splicing and protein expression in the living human brain. PLoS One. 2025;20:e0332651 https://doi.org/10.1371/journal.pone.0332651
16. Rodriguez de los Santos M, Kopell BH, Buxbaum Grice A, Ganesh G, Yang A, Amini P, et al. Divergent landscapes of A-to-I editing in postmortem and living human brain. Nature Communications. 2024;15:5366 https://doi.org/10.1038/s41467-024-49268-z
17. Batten, SR, Bang, D, Kopell, BH, Davis, AN, Heflin, M, Fu, Q et al. Dopamine and serotonin in human substantia nigra track social context and value signals during economic exchange. Nat Hum Behav 2024. https://doi.org/10.1038/s41562-024-01831-w
18. Gazestani V, Kamath T, Nadaf NM, Dougalis A, Burris SJ, Rooney B, et al. Early Alzheimer's disease pathology in human cortex involves transient cell states. Cell. 2023;186:4438–53 e4423. https://doi.org/10.1016/j.cell.2023.08.005
19. Berto S, Fontenot MR, Seger S, Ayhan F, Caglayan E, Kulkarni A, et al. Gene-expression correlates of the oscillatory signatures supporting human episodic memory encoding. Nat Neurosci. 2021;24:554–64. https://doi.org/10.1038/s41593-021-00803-x
20. Miocinovic S, Somayajula S, Chitnis S, Vitek JL. History, applications, and mechanisms of deep brain stimulation. JAMA Neurol. 2013;70:163–71. https://doi.org/10.1001/2013.jamaneurol.45
21. Vornholt, E, Liharska, LE, Cheng, E, Hashemi, A, Park, YJ, Ziafat, K *et al*. Characterizing cell type specific transcriptional differences between the living and postmortem human brain. *medRxiv*, 2024.2005.2001.24306590 [Preprint]. 2024. https://doi.org/10.1101/2024.05.01.24306590
22. Sands LP, Jiang A, Liebenow B, DiMarco E, Laxton AW, Tatter SB, et al. Subsecond fluctuations in extracellular dopamine encode reward and punishment prediction errors in humans. Sci Adv. 2023;9:eadi4927 https://doi.org/10.1126/sciadv.adi4927
23. Phillips PE, Stuber GD, Heien ML, Wightman RM, Carelli RM. Subsecond dopamine release promotes cocaine seeking. Nature. 2003;422:614–8. https://doi.org/10.1038/nature01476
24. Moran RJ, Kishida KT, Lohrenz T, Saez I, Laxton AW, Witcher MR, et al. The Protective Action Encoding of Serotonin Transients in the Human Brain. Neuropsychopharmacology. 2018;43:1425–35. https://doi.org/10.1038/npp.2017.304
25. Kishida KT, Sandberg SG, Lohrenz T, Comair YG, Saez I, Phillips PE, et al. Subsecond dopamine detection in human striatum. PLoS One. 2011;6:e23291 https://doi.org/10.1371/journal.pone.0023291
26. Kishida KT, Saez I, Lohrenz T, Witcher MR, Laxton AW, Tatter SB, et al. Subsecond dopamine fluctuations in human striatum encode superposed error signals about actual and counterfactual reward. Proc Natl Acad Sci USA. 2016;113:200–5. https://doi.org/10.1073/pnas.1513619112
27. Clark JJ, Sandberg SG, Wanat MJ, Gan JO, Horne EA, Hart AS, et al. Chronic microsensors for longitudinal, subsecond dopamine detection in behaving animals. Nat Methods. 2010;7:126–9. https://doi.org/10.1038/nmeth.1412
28. Bang D, Kishida KT, Lohrenz T, White JP, Laxton AW, Tatter SB, et al. Sub-second Dopamine and Serotonin Signaling in Human Striatum during Perceptual Decision-Making. Neuron. 2020;108:999–1010 e1016. https://doi.org/10.1016/j.neuron.2020.09.015
29. Crockett MJ, Clark L, Tabibnia G, Lieberman MD, Robbins TW. Serotonin modulates behavioral reactions to unfairness. Science. 2008;320:1739 https://doi.org/10.1126/science.1155577
30. Crockett MJ, Clark L, Hauser MD, Robbins TW. Serotonin selectively influences moral judgment and behavior through effects on harm aversion. Proc Natl Acad Sci USA. 2010;107:17433–8. https://doi.org/10.1073/pnas.1009396107
31. Cacciola A, Milardi D, Anastasi GP, Basile GA, Ciolli P, Irrera M, et al. A Direct Cortico-Nigral Pathway as Revealed by Constrained Spherical Deconvolution Tractography in Humans. Front Hum Neurosci. 2016;10:374 https://doi.org/10.3389/fnhum.2016.00374
32. Handfield-Jones N. Connectomic Analysis of Substantia Nigra Pars Compacta and Ventral Tegmental Area Projections to the Striatum and Cortex. Canada: The University of Western Ontario; 2019.
33. Storey JD, Tibshirani R. Statistical significance for genomewide studies. Proc Natl Acad Sci USA. 2003;100:9440–5. https://doi.org/10.1073/pnas.1530509100
34. Kanehisa M, Sato Y, Kawashima M. KEGG mapping tools for uncovering hidden features in biological data. Protein Sci. 2022;31:47–53. https://doi.org/10.1002/pro.4172
35. Zheng ZS, Monti MM. Cortical and thalamic connections of the human globus pallidus: Implications for disorders of consciousness. Front Neuroanat. 2022;16:960439 https://doi.org/10.3389/fnana.2022.960439
36. Aron AR, Herz DM, Brown P, Forstmann BU, Zaghloul K. Frontosubthalamic Circuits for Control of Action and Cognition. J Neurosci. 2016;36:11489–95. https://doi.org/10.1523/JNEUROSCI.2348-16.2016
37. Wiest C, Torrecillos F, Pogosyan A, Bange M, Muthuraman M, Groppa S, et al. The aperiodic exponent of subthalamic field potentials reflects excitation/inhibition balance in Parkinsonism. Elife. 2023;12:e82467 https://doi.org/10.7554/eLife.82467
38. Tripathy SJ, Toker L, Li B, Crichlow CL, Tebaykin D, Mancarci BO, et al. Transcriptomic correlates of neuron electrophysiological diversity. PLoS Comput Biol. 2017;13:e1005814 https://doi.org/10.1371/journal.pcbi.1005814
39. Bomkamp C, Tripathy SJ, Bengtsson Gonzales C, Hjerling-Leffler J, Craig AM, Pavlidis P. Transcriptomic correlates of electrophysiological and morphological diversity within and across excitatory and inhibitory neuron classes. PLoS Comput Biol. 2019;15:e1007113 https://doi.org/10.1371/journal.pcbi.1007113
40. Karczewski KJ, Francioli LC, Tiao G, Cummings BB, Alfoldi J, Wang Q, et al. The mutational constraint spectrum quantified from variation in 141,456 humans. Nature. 2020;581:434–43. https://doi.org/10.1038/s41586-020-2308-7
41. Lui JH, Nguyen ND, Grutzner SM, Darmanis S, Peixoto D, Wagner MJ, et al. Differential encoding in prefrontal cortex projection neuron classes across cognitive tasks. Cell. 2021;184:489–506 e426. https://doi.org/10.1016/j.cell.2020.11.046
42. Pai AA, Luca F. Environmental influences on RNA processing: Biochemical, molecular and genetic regulators of cellular response. Wiley Interdiscip Rev RNA. 2019;10:e1503 https://doi.org/10.1002/wrna.1503
43. International Schizophrenia, C., Purcell, SM, Wray, NR, Stone, JL, Visscher, PM, O'Donovan, MC et al. in *Nature* Vol. 460 748 (2009).
44. Ismail Fawaz H, Lucas B, Forestier G, Pelletier C, Schmidt DF, Weber J, et al. Inceptiontime: Finding alexnet for time series classification. Data Mining and Knowledge Discovery. 2020;34:1936–62.
45. Donoghue T, Haller M, Peterson EJ, Varma P, Sebastian P, Gao R, et al. Parameterizing neural power spectra into periodic and aperiodic components. Nat Neurosci. 2020;23:1655–65. https://doi.org/10.1038/s41593-020-00744-x
46. Eyre TA, Ducluzeau F, Sneddon TP, Povey S, Bruford EA, Lush MJ. The HUGO Gene Nomenclature Database, 2006 updates. Nucleic Acids Res. 2006;34:D319–321. https://doi.org/10.1093/nar/gkj147
47. Benjamini Y, Drai D, Elmer G, Kafkafi N, Golani I. Controlling the false discovery rate in behavior genetics research. Behav Brain Res. 2001;125:279–84. https://doi.org/10.1016/s0166-4328(01)00297-2
48. Wu P, Gifford A, Meng X, Li X, Campbell H, Varley T, et al. Mapping ICD-10 and ICD-10-CM codes to phecodes: workflow development and initial evaluation. JMIR Med Inform. 2019;7:e14325 https://doi.org/10.2196/14325
49. Wei WQ, Bastarache LA, Carroll RJ, Marlo JE, Osterman TJ, Gamazon ER, et al. Evaluating phecodes, clinical classification software, and ICD-9-CM codes for phenome-wide association studies in the electronic health record. PLoS One. 2017;12:e0175508 https://doi.org/10.1371/journal.pone.0175508
50. Landi I, Kaji DA, Cotter L, Van Vleck T, Belbin G, Preuss M, et al. Prognostic value of polygenic risk scores for adults with psychosis. Nat Med. 2021;27:1576–81. https://doi.org/10.1038/s41591-021-01475-7
51. Forrest IS, Chaudhary K, Vy HMT, Petrazzini BO, Bafna S, Jordan DM, et al. Population-based penetrance of deleterious clinical variants. JAMA. 2022;327:350–9. https://doi.org/10.1001/jama.2021.23686
52. Ritchie ME, Phipson B, Wu D, Hu Y, Law CW, Shi W, et al. limma powers differential expression analyses for RNA-sequencing and microarray studies. Nucleic Acids Res. 2015;43:e47 https://doi.org/10.1093/nar/gkv007

ACKNOWLEDGEMENTS

The Living Brain Project study participants are commended for their important role in science. The following centers, programs, departments and institutes within the Icahn School of Medicine at Mount Sinai supported the work: Charles Bronfman Institute of Personalized Medicine; Department of Neurosurgery; Department of Genetics and Genomic Sciences; Department of Psychiatry; Department of Neuroscience; Department of Medicine; Friedman Brain Institute; Center for Neuromodulation; Center for Computational Psychiatry; Nash Family Center for Advanced Circuit Therapeutics. The following centers, programs, departments and institutes within the Virginia Tech supported the work: Fralin Biomedical Research Institute; Department of Physics. The following centers, programs, departments and institutes within the Aarhus University supported the work: Center of Functionally Integrative Neuroscience. The following centers, programs, departments and institutes within the University College London supported the work: Wellcome Centre for Human Neuroimaging. The following centers, programs, departments and institutes within Oxford supported the work: Department of Experimental Psychology. The following centers, programs, departments and institutes within Rice University supported the work: Department of Statistics. The following centers, programs, departments and institutes within Wake Forest supported the work: Department of Translational Neuroscience; Department of Neurosurgery. Thank you to Dr. Xiaosi Gu and her team (Arianna Neal Davis, Ofer Perl, Qixiu Fu, Matthew Heflin) for helping with the voltammetry data collection.

AUTHOR CONTRIBUTIONS

AWC and BHK conceived and designed the study. Funding for the work was acquired by AWC, BHK, EES, GNN, PRM, IS. Participant enrollment was performed by AWC, BHK, AH, LW, KZ, HS, LML, BS, EC, YJP, EM, and JS. LIV samples were obtained during DBS procedures by BHK. Procedures related to RNA sequencing data generation and analysis were performed by AWC, NDB, LEL, YJP, EC, LW, CF, JSJ, NB, EV, RCT, and MSB. Procedures related to electrophysiology data generation and analysis were performed by BHK, AWC, AV, AL, TL, SQ, AA, SRB, DB, LSB, TT, JPW, MV, BH, MF, KTK, IS, and PRM. The report was primarily written by AWC and LEL. All other authors contributed to writing specific parts of the report. Figures and tables were made by AWC and LEL.

FUNDING

National Institute of Aging R01AG069976 The Michael J. Fox Foundation 18232.

COMPETING INTERESTS

BHK is a consultant for Medtronic and Abbott.

ADDITIONAL INFORMATION

Supplementary information The online version contains supplementary material available at https://doi.org/10.1038/s41380-025-03420-3.

Correspondence and requests for materials should be addressed to Alexander W. Charney.